Synthesis of Hybrid Organic−Inorganic Materials from Interpenetrating Polymer Network Chemistry

C. L. Jackson,* B. J. Bauer, A. I. Nakatani, and J. D. Barnes

Materials Science and Engineering Laboratory, National Institute of Standards and Technology, Gaithersburg, Maryland 20899

Received September 7, 1995. Revised Manuscript Received December 18, 1995[⊗]

Organic−inorganic interpenetrating polymer networks were synthesized with an SiO_2 phase made by sol−gel chemistry and the organic phase made from poly(2-hydroxyethyl acrylate). The resultant morphologies were characterized by small-angle scattering and electron microscopy. When the vinyl polymerization is more rapid than the sol−gel reaction, gross phase separation occurs giving a heterogeneous structure. For comparable rates of the two polymerizations, the specimens have a dendritic morphology on the scale of 0.5 μm. The more rapid formation of the silica phase relative to the organic network produces rigid and optically transparent materials, with a finely divided structure as seen by transmission electron microscopy. The glass content of these materials is about 0.15 g/g and the sizes of the SiO_2-rich domains are 100 Å or less. Addition of tetrakis(2-(acryloxy)ethoxy)silane was also studied and found to promote phase mixing between the organic and inorganic phases.

Introduction

The preparation of a composite from two materials with vastly different physical properties is a recurrent concept in materials science, as few pure materials fulfill the strength, design, and cost requirements of modern applications. For example, polymeric resins are often "filled" with silica to improve the thermal, mechanical, and electrical properties. Processing materials such as glass and polymer together, however, is technically difficult because of the need to ensure uniformity of the dispersion and good interfacial adhesion between the matrix and filler.[1] An effort to circumvent these technical difficulties has resulted in the recent development of alternative synthetic routes to composite materials. For example, the chemical preparation of inorganic oxides such as SiO_2 within a polymer matrix has produced a new breed of "nanocomposite" structures, to be discussed in this work.

The design of nanocomposites has been focused on the in situ preparation of sol−gel glasses and organic polymers.[2−4] In these hybrids of organic and inorganic materials a very fine-scale morphology can be produced, resulting in optically transparent materials. Because the glass content can be varied over a wide range, many applications for these new materials have been forecast, from impact resistant glasses and waveguides to scratch-resistant coatings and reinforced adhesives. Materials produced by this method have strong parallels with biological composite materials such as teeth and bones, in which mineral particles are grown in situ within a polymeric matrix, as reviewed recently by Calvert and Mann.[5]

The sol−gel method produces a finely divided morphology of SiO_2 under mild synthetic conditions. The overall reaction is a hydrolysis of a tetrafunctional silicate, such as tetraethyl orthosilicate (TEOS), to form SiO_2 and an alcohol byproduct, under either acidic or basic conditions. An organic solvent is usually necessary since most orthosilicates are immiscible with water. This type of chemistry has been utilized extensively to form porous silica structures, which initially are prepared as an SiO_2 network in solvent. When the solvent is removed, aerogels or xerogels are formed.[6] Organic−inorganic composites have been made by synthesizing the SiO_2 phase through sol−gel chemistry in solutions of preformed linear polymer,[7−9] cross-linked polymer,[10] or oligomers.[11,12]

More recently organic−inorganic composites have been prepared by Novak and co-workers[13−15] using interpenetrating polymer network (IPN) chemistry. If the solvent is a polymerizable monomer, then two independent reactions can take place: the sol−gel reaction will form an inorganic component, and the organic reaction will form an organic polymer. The resulting material is an IPN made up of organic and inorganic phases. The chemistry involves hydrolysis of an orthosilicate:

$$Si(OR)_4 + 2H_2O + \text{monomer} + \text{solvent} \rightarrow SiO_2 + 4ROH + \text{polymer} + \text{solvent}$$

The volatile solvent can be eliminated if the monomer

[⊗] Abstract published in *Advance ACS Abstracts,* February 1, 1996.

(1) McGarry, F. J. *Annu. Rev. Mater. Sci.* **1994**, *24*, 63.
(2) Schmidt, H. *J. Non-Cryst. Solids* **1985**, *73*, 681.
(3) Schmidt, H. K. In *Chemical Processing of Advanced Materials*; Hench, L. L., West, J. K., Eds.; Wiley: New York, 1992.
(4) Novak, B. M. *Adv. Mater.* **1993**, *5*, 422.
(5) Calvert, P.; Mann, S. *J. Mater. Sci.* **1988**, *23*, 3801.
(6) Fricke, J.; Emmerling, A. *Struct. Bonding* **1992**, *77*, 37.
(7) Landry, C. J. T.; Coltrain, B. K.; Landry, M. R.; Fitzgerald, J. J.; Long, V. K. *Macromolecules* **1993**, *26*, 3702.
(8) Coltrain, B. K.; Ferrar, W. T.; Landry, C. J. T.; Molaire, T. R.; Zumbulyadis, N. *Chem. Mater.* **1992**, *4*, 358.
(9) Coltrain, B. K.; Landry, C. J. T.; O'Reilly, J. M.; Chamberlain, A. M.; Rakes, G. S.; Sedita, J. S.; Kelts, L. W.; Landry, M. R.; Long, V. K. *Chem. Mater.* **1993**, *5*, 1445.
(10) Mark, J. E.; Ning, Y.-P.; Jiang, C.-Y.; Tang, M.-Y.; Roth, W. C. *Polymer* **1985**, *26*, 2069.
(11) Huang, H. H.; Orler, B.; Wilkes, G. L. *Macromolecules* **1987**, *20*, 1322.
(12) Wang, S.; Ahmad, Z.; Mark, J. E. *Chem. Mater.* **1994**, *6*, 943.
(13) Novak, B. M.; Davies, C. *Macromolecules* **1991**, *24*, 5481.
(14) Ellsworth, M. W.; Novak, B. M. *Chem. Mater.* **1993**, *5*, 839.
(15) Ellsworth, M. W.; Novak, B. M. *J. Am. Chem. Soc.* **1991**, *113*, 2756.

0897-4756/96/2808-0727$12.00/0

acts as a good solvent for the sol−gel components. Also, essentially "nonshrinking" composites can be prepared if the R group can also polymerize with the organic monomer, since no mass loss occurs due to elimination of volatile components from the reaction mixture. Composites with glass contents up to 75 wt % were recently prepared by using a modified in situ synchronous polymerization route and highly branched poly(silicic acid) samples.[14]

IPNs of two organic polymers are usually formed by two independent polymerizations that may be either sequential or simultaneous. The result is a sample that is microscopically phase separated but macroscopically uniform.[16] Although the two monomers or the monomer−polymer combination initially form a single phase, phase separation occurs at some point in the polymerization and a finely divided morphology results. If grafting between the components of IPNs is possible, this greatly affects the point of the phase separation and the ultimate morphology. Studies of IPNs made from polymers that form miscible blends have shown that while the cross-linking reaction can strongly promote phase separation,[17] the grafting reaction tends to inhibit phase separation.[18]

The two-phase morphology formed with IPN chemistry is often significantly different from that of a simple physical mixture of the two components. In particular, co-continuous morphologies can yield materials with bulk mechanical properties that are dominated by the minor component.[19] In contrast, conventional silica-filled polymer composites are made by physically mixing preformed silica into polymers, which tends to produce properties that either are dominated by the matrix polymer or are averages of the properties of two components. For silica-filled polymers formed by swelling an organic polymer or network in orthosilicate monomers and subsequently polymerizing by the sol−gel method,[7,10,11] the silica is usually more finely dispersed than a physical mixture but the morphology often contains discrete particles.[10] We have recently prepared materials in this manner using epoxy resin as the matrix.[20]

The morphology of organic−inorganic IPNs synthesized with an organic polymer phase made from poly(2-hydroxyethyl acrylate) (HEA) and an inorganic SiO_2 phase made by a sol−gel hydrolysis reaction are the subject of this report. An "ungrafted" series of IPNs (HEA series) was prepared by in situ polymerization with the relative amounts of sol−gel catalyst and vinyl free radical initiator as the variable, resulting in different rates of polymerization for the two phases. The amount of phase separation between the organic and inorganic phase was found to greatly influence the morphology within this series as described in a preliminary report.[21] A "grafted" series of IPNs was also synthesized (B series), using the orthosilicate monomer of tetrakis(2-(acryloxy)ethoxy)silane (TAEOS), to determine whether chemical bonds initially present between the phases inhibit phase separation between the organic and inorganic phases. The terms "ungrafted" and "grafted" in this context are relative because of the possibility of hydrolysis and interchange in both reaction mixtures. In the "ungrafted" series, the organic polymer contains hydroxyls which can exchange with the ethyl groups of the TEOS, producing some grafts during the reaction. In the "grafted" series, the Si−O−C bonds can be hydrolyzed to cleave the graft at higher conversions. The presence of the ethyl groups on the TEOS in the "ungrafted" series means that overall there are initially far fewer bonds between the organic and inorganic phases. We present small-angle scattering and transmission electron microscopy (TEM) results to demonstrate how the synthetic pathway affects the resulting structures. The experimental results suggest that the ethyl group on TEOS in the "ungrafted" series does not exchange with the HEA to the extent present when starting with TAEOS, if even partial hydrolysis of the "grafted" series occurs.

Table 1. Catalyst Weight Ratios and SiO_2 Content of Organic−Inorganic IPNs

sample ID	HF/TEOS or HF/TAEOS[a]	HF/benzoyl peroxide[b]	SiO_2 by TGA[c]
HEA-1	0.0004	0.04	0.10 to 0.23
HEA-2	0.0025	0.25	0.12
HEA-3	0.0026	0.26	0.15
HEA-4	0.0107	1.06	0.16
HEA-5	0.0270	2.67	0.15
B-2	0.0001	0.01	0.05
B-7	0.0036	0.36	0.05

[a] An error of ±0.0001 is estimated from the gravimetric measurements. [b] An error of ±0.01 is estimated from the gravimetric measurements. [c] An error estimate of ±0.01 is estimated from multiple measurements.

Experimental Section

The "ungrafted" HEA series was prepared by adding a water/hydrofluoric acid (HF) mixture to tetraethyl orthosilicate (TEOS) in the presence of an organic monomer, 2-hydroxyethyl acrylate (HEA). The TEOS to HEA weight ratio was 0.79 in all cases. The free radical initiator for the vinyl polymerization was benzoyl peroxide, added at 0.008 g/g with respect to the acrylate. The molar ratio of water to TEOS was 4:1. The HEA acted as a cosolvent forming homogeneous solutions upon mixing. The samples were purged with nitrogen and placed in a 70 °C dry bath to complete the SiO_2 hydrolysis and HEA polymerization. After solidification, the ethanol which formed during the hydrolysis reaction rose to the surface with a small amount of TEOS. After evaporation of the ethanol, a slight SiO_2 layer remained on the surface, which was removed before analysis. Table 1 lists the experimental conditions.

The "grafted" B-series was prepared by using equal weights of HEA and TAEOS and treating as in the case of the TEOS system. The TAEOS was synthesized by adding 0.1 mol of silicon tetrachloride to 0.44 mol of HEA in 200 mL of dry toluene with excess poly(4-vinylpyridine) as an acid trap. The product was filtered, the volatile components were stripped off in vacuum, and the residual liquid TAEOS was recovered. For the subsequent synthesis of the B-series IPNs, the benzoyl peroxide to monomer weight ratio was 0.01. A variety of HF contents were used with HF to TAEOS ratios between 0.0001 and 0.01 (Table 1).

Thermogravimetric analysis (TGA) was used to determine the SiO_2 content of the specimens and the decomposition

(16) Sperling, L. H. *Interpenetrating Polymer Networks*; Adv. Chem. Ser. **1994**, *239*, 3.
(17) Bauer, B. J.; Briber, R. M.; Han, C. C. *Macromolecules* **1989**, *22*, 940.
(18) Bauer, B. J.; Briber, R. M.; Dickens, B. *Interpenetrating Polymer Networks*; Adv. Chem. Ser. **1994**, *239*.
(19) Chiang, C. K.; Bauer, B. J.; Briber, R. M.; Davis, G. T. *Polymer* **1987**, *28*, 34.
(20) Bauer, B. J.; Liu, D.-W.; Jackson, C. L.; Barnes, J. D. *Polym. Adv. Technol.*, in press.
(21) Jackson, C. L.; Bauer, B. J.; Barnes, J. D. *ACS PMSE Prepr.* **1994**, *71*, 85.

Table 2. Sample Characteristics from TEM Images

sample	physical appearance	domain size, Å	domain uniformity	observations from TEM
HEA-1	slightly opaque, rubbery, tacky	300−3000	very poor	grossly phase separated, fractal
HEA-2	slightly opaque, rubbery	200−2000	good	fractal structure, diffuse edges
HEA-3	slightly opaque, tougher than HEA-2	600−2000	good	fractal structure, rounded edges
HEA-4	optically clear, rigid and tough	<100	very good	very fine texture
HEA-5	optically clear, rigid and tough	<100	very good	very fine texture
B-2	optically clear, tough	100−200	very good	mottled texture, very diffuse edges
B-7	optically clear, tough	<100	very good	very fine texture

temperature profile. A Perkin-Elmer TGA 7[22] was used to heat approximately 5 mg of the sample at 10 °C/min from 30 to 800 °C in an air atmosphere.

Small-angle X-ray scattering (SAXS) was performed at the NIST Polymers Division SAXS facility.[23] Scattering was done at room temperature in vacuo using Cu Kα radiation (1.54 Å wavelength). Scattered X-rays were collected over a two-dimensional detector. The data were corrected for dark current, scattering from the empty beam, and transmission. The results were circularly averaged and are expressed in relative intensity units. Small-angle neutron scattering (SANS) was performed at the 30 m NSF instrument at NIST.[24] A wavelength of 7 Å was used with a wavelength spread of $\Delta\lambda/\lambda = 0.31$ and a sample-to-detector distance of 1530 cm. Data were corrected for the empty beam, blocked beam, and incoherent scattering. A baseline was estimated[25] by plotting Iq^4 vs q^4 and taking the slope of the line at q values >0.2 Å^{-1}.

For the transmission electron microscopy (TEM) studies, a bulk specimen of each sample was cut to a size of 1 mm × 1 mm × 2 mm and mounted on a pin for the appropriate specimen holder for the cryochamber of the microtome. Ultrathin sections were cryomicrotomed using a diamond knife at temperatures from −20 to −80 °C, depending on the specimen character. The quality of the thin sections for these materials was very sensitive to the cutting temperature and had to be adjusted to within ±10 °C. If the temperature was too low, the specimen tended to form a powder rather than a slice. The sections were transferred dry to carbon-coated Cu grids of 200 mesh. The nominal section thickness was 600−900 Å. The sections were imaged on a Philips 400T at 120 kV.[22] The contrast between the silicon-containing phase and the polymer was sufficient for imaging, and no staining was required.

Results and Discussion

1. Synthesis. HF was used as catalyst for the TEOS since it is known to produce clear, uniform gels at rates similar to those of vinyl polymerizations.[26] The amount of HF catalyst was the variable used to empirically change the relative rates of polymerization. In sol−gel chemistry, it is well-known that the type of catalyst strongly affects the hydrolysis and condensation reaction and the ultimate morphology.[4,26,27] Therefore, our results are specific to HF catalysis of orthosilicates and may not be generally applicable to other catalyst systems. The possibility of extensive side reactions in this mixture, such as the hydrolysis of the ester linkage in the HEA or addition of HF across the double bond of the monomer, are considered to be minimal based on the literature of these well-studied systems. The hydrolysis of acrylate esters at a pH of 7 or less is quite slow[28,29] compared to basic hydrolysis and emulsion polymerizations of acrylate esters are usually carried out under neutral or acidic conditions.[30,31] The addition of halogen acids to both acrylate and methacrylate esters is reported to occur in organic solvents such as hexane or CCl_4 but not in solvents such as water or methanol[29,32,33] and not from dilute aqueous solutions of hydrochloric acid.[30]

The synthesis of the HEA series of "ungrafted" polymers was conducted according to the catalyst/free radical initiator ratios (HF/benzoyl peroxide) and HF/TEOS ratios given in Table 1. The resultant materials exhibited a wide range of structures, as summarized in Table 2. Simple visual inspection of the samples HEA-1 through HEA-5 showed large differences, from slightly opaque, rubbery samples in HEA-1 and HEA-2, to optically clear, rigid, and tough samples in HEA-4 and HEA-5. When the free radical polymerization of the acrylate groups was fast with respect to the sol−gel reaction rate (HEA-1), visible phase separation occurred during the polymerization. TGA scans taken from pieces of HEA-1 in different regions of the sample varied between 0.10 and 0.23 g/g of SiO_2, as given in Table 1. This suggests that macroscopic heterogeneities exist within the sample. The samples with higher HF/benzoyl peroxide ratios formed homogeneous gels. The pyrolysis products of HEA-2 through HEA-5 were the same size and shape as the original specimens, suggesting the SiO_2 phase was continuous even though it only represented about 0.15 g/g or 6% volume fraction of the sample.

The synthesis of the "grafted" samples in the B series was done according to the catalyst ratios (HF/benzoyl peroxide) and HF/TAEOS ratios listed in Table 1. The SiO_2 content was near 0.05 g/g in all cases. The lower SiO_2 content was caused by the lower initial silicon content of the starting monomer mixture of the B series compared to the HEA series and the fact that the HEA series lost volatile ethanol. As summarized in Table 2, the B series were all optically clear, tough and flexible.

2. Small-Angle Scattering. A double logarithmic plot of SAXS and SANS intensity, I, versus the scattering vector, q, for the HEA series is shown in Figure 1. The scattering vector is defined as $q = 4\pi(\sin(\theta/2))/\lambda$,

(22) Certain commercial materials and equipment are identified in this paper in order to specify adequately the experimental procedure. In no case does such identification imply recommendation by the National Institute of Standards and Technology nor does it imply that the material or equipment identified is necessarily the best available for this purpose.

(23) Barnes, J. D.; Mopsik, F. *46th Annu. Techn. Conf. Proc., Soc. Plastics Eng.* **1988**, 1179.
(24) Prask, H. J.; Rowe, M.; Rush, J. J.; Schroeder, I. G. *J. Res. Natl. Inst. Stand. Tech.* **1993**, *98*, 1.
(25) Murthy, N. S.; Orts, W. J. *ACS PMSE Prepr.* **1994**, *71*, 293.
(26) Pope, E. J. A.; Mackenzie, J. D. *J. Non-Cryst. Solids* **1986**, *87*, 185.
(27) Schaefer, D. W. *MRS Bull.* **1988**, *Feb*, p. 22.
(28) Williams, T.; Sudborough, J. J. *J. Am. Chem. Soc.* **1912**, *101*, 412.
(29) Riddle, E. H. *Monomeric Acrylic Esters*; Reinhold Publishing Corp.: New York, 1954; p 51.
(30) Mast, W. C.; Fisher, C. H. *Ind. Eng. Chem.* **1949**, *41* (4), 790.
(31) Hamilton, C. J.; Tighe, B. J. In *Comprehensive Polymer Science*; Eastmond, G. C., et al., Eds.; Pergammon Press: Oxford, 1989; Vol. 3, Chapter 20.
(32) Price, C. C.; Coyner, E. C. *J. Am. Chem. Soc.* **1940**, *62*, 1306.
(33) Moureu, C.; Murat, M.; Tampier, L. *Comptes Rendus* **1921**, *172*, 1267.

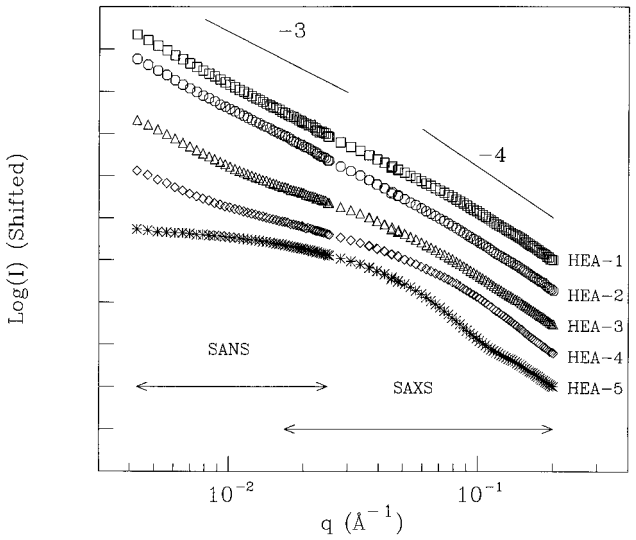

Figure 1. log(I) versus log(q) from SANS and SAXS data for organic−inorganic IPNs in the "ungrafted" HEA series: HEA-1, □; HEA-2, ○, HEA-3, △; HEA-4, ◇; HEA-5, ∗. Solid lines illustrate slopes of −3 and −4, for reference.

Table 3. Scattering Analysis of HEA and B Series

sample	volume/ surface, (Å)	interfacial thickness T (Å)	fractal power law	power law range (Å)
HEA-1	>400	*a*	∼3.1	60−600
HEA-2	>400	*a*	∼3.1	60−600
HEA-3	>200	*a*		
HEA-4	120 ± 10	4 ± 2		
HEA-5	140 ± 10	9 ± 2		
B-2	no Porod region	no Porod region	∼2.4	30−300
B-7	no Porod region	no Porod region	∼2.0	30−100

[a] An interfacial region could not be measured.

where θ is the scattering angle and λ is the wavelength of the incident beam. Both SANS and SAXS data are shown in arbitrary intensity units and are shifted vertically for clarity. Samples HEA-1 and HEA-2 have a constant power law over a considerable q range, with a slope of approximately −3.1. Over a considerable size scale, these samples exhibit fractal structure[27,34] with a range of self-similar structure between $2\pi/q_{min}$ and $2\pi/q_{max}$, over the power law range listed in Table 3. At higher scattering angle, the slopes in the Porod region, $qD \gg 1$, where D is the characteristic domain size of the two phase morphology, are closer to $\partial \log(I)/\partial \log(q) = -4$. Thus for the entire series of samples from HEA-1 to HEA-5, this indicates strong phase separation into domains with little mixing of the phases. Samples HEA-4 and HEA-5 have power law scattering <-4, suggesting that a broader interfacial area may exist. We do not observe a scattering maxima for these materials, such as was described by Landry et al.[34] for hybrid materials made via a different route.

Small-angle scattering from two-phase materials is generally characterized as having contributions from the domain structures of the two phases, the interfacial regions between the domains, and mixtures of the two components within the phases. In cases where contributions from mixtures of components within the phases is negligible, data analysis in the Porod region can give characteristic phase size and interfacial thickness.[35−37] The scattering from a two-phase mixture with volume V, surface area S, interfacial area A, volume fraction of one component ϕ_i, interfacial thickness T, and scattering vector, $q = 4\pi \sin(\theta)/\lambda$ has an asymptotic form:

$$\frac{q^4 I(q)}{\int_0^\infty q^2 I(q)\, dq} = \frac{S/V \exp(-T^2 q^2)}{\pi\phi\,(1-\phi)} \qquad (1)$$

In this form the scattered intensity, I, is in both numerator and denominator, so that absolute intensity calibration is not necessary. The volume to surface ratio (V/S) is related to characteristic phase sizes, with l_1 and l_2 the average chord size of phases 1 and 2, with l_i equal to $4\phi_i V/S$.[37] The interfacial thickness, T, is characteristic of the zone of mixing between the two phases.

The invariant $\int_0^\infty q^2 I(q)\, dq$, needs to be calculated over all q, so extrapolations need to be made outside of the range of experimental data. In this case the extrapolation was made in the low-q range of

$$I(q) = I(0)/(1 + \xi^2 q^2)^2 \qquad (2)$$

which applies to an exponential correlation function,[38] where ξ is the correlation length. In cases where power law scattering from a fractal type of structure extends beyond the lowest measured q value, this function underestimates the invariant integration at low q, and therefore the volume-to-surface ratio represents a minimum value.

Table 3 summarizes the SAXS and SANS data of the HEA series samples using the above analysis of characteristic phase size and interfacial thickness. Equation 1 was used to fit the data by plotting log Iq^4 versus q^2. A linear fit through the high-q data was used to obtain the V/S ratio and interfacial thickness. Samples HEA-1 through HEA-3 had no discernible slope; thus an interfacial region could not be estimated using this method. These were the specimens with the fastest relative vinyl polymerization rate and the largest domain sizes. The domain sizes for HEA-1 and HEA-2 were estimated as >400 Å from this analysis. As the HF concentration was increased, the sol−gel reaction rate increased so that the reaction rates become comparable and the SiO_2 domains became smaller. For example, V/S ratios for HEA-4 and HEA-5 were estimated to be 120 and 140 Å, respectively. The interfaces also become thicker under these synthetic conditions and can be more reasonably measured by this analysis. For HEA-4 and HEA-5, the interfacial thicknesses were estimated to be 4 ± 2 and 9 ± 2 Å, respectively.

The SAXS and SANS scattering intensity versus q from the B series samples is shown in Figure 2. In this case, the scattering never approaches a region with a −4 power law, so a Porod analysis is impossible. The B series have power laws of $\partial \log(I)/\partial \log(q) = -2.4$ and −2.0 for samples B-2 and B-7, respectively, indicating extensive mixing of the two components and weak phase separation. These values are listed in Table 3, along with the data for the HEA series for comparison. A limiting power law of −2 has been observed in the case

(34) Landry, M. R.; Coltrain, B. K.; Landry, C. J. T.; O'Reilly, J. M. *J. Polym. Sci., Polym. Phys. Ed.* **1995**, *33*, 637.
(35) Porod, G. *Kolloid Z.* **1951**, *124*, 83.
(36) Debye, P.; Bueche, A. M. *J. Appl. Phys.* **1949**, *20*, 518.
(37) Porod, G. *Kolloid Z.* **1952**, *125*, 51.
(38) Roe, R.-J. *Encyclopedia of Polymer Science and Engineering*; Wiley-Interscience: New York, 1988; Vol. 17, pp 981−986.

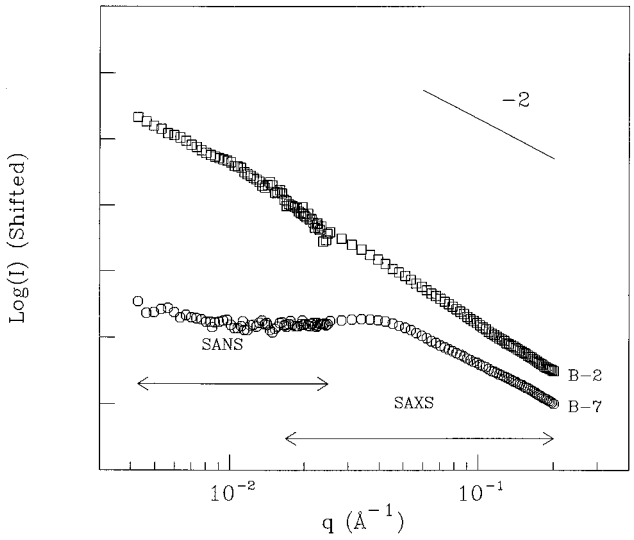

Figure 2. log(*I*) versus log(*q*) from SANS and SAXS data for the "grafted" B series including B-2, □; B-7, ○. Solid line illustrates a slope of −2.

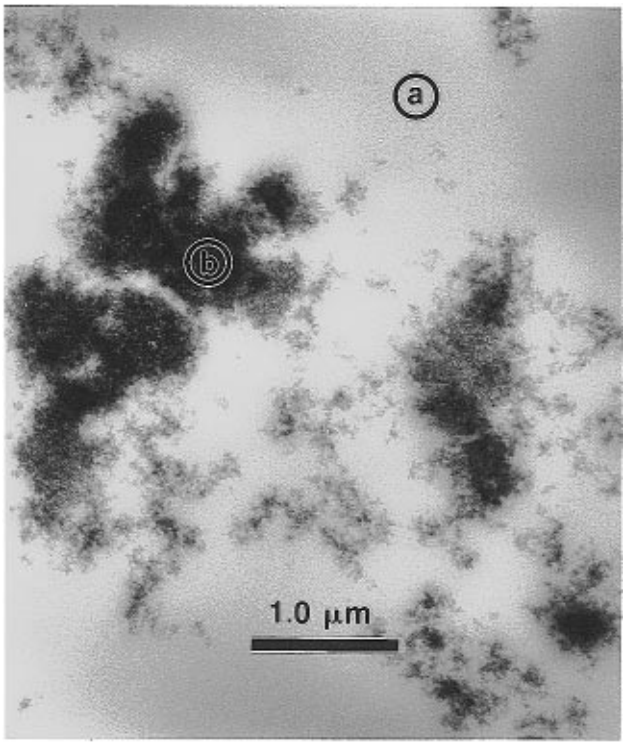

Figure 3. Typical morphology of specimen HEA-1, as seen by transmission electron microscopy (TEM). The organic regions appear light, labeled "a", and the inorganic, SiO_2-rich regions appear dark, labeled "b". At this catalyst ratio, the vinyl polymerization occurs first, resulting in nonuniform dispersion of the subsequently polymerized sol−gel component.

of miscible polymer blends where intimate mixing of the two components occurs.[18] While both B samples have higher *q* scattering power laws near −2, sample B-2 has an extended power law range down to $q = 0.004$ Å^{-1}, while sample B-7 has very weak scattering at low *q* with a weak peak at 0.035 Å^{-1}. The limiting power law slopes from the scattering data indicate that the "grafted" series is more phase mixed than the "ungrafted" series and suggest that the different reaction pathways have a controlling effect on the final morphology, even if hydrolysis and exchange reactions occur to some extent.

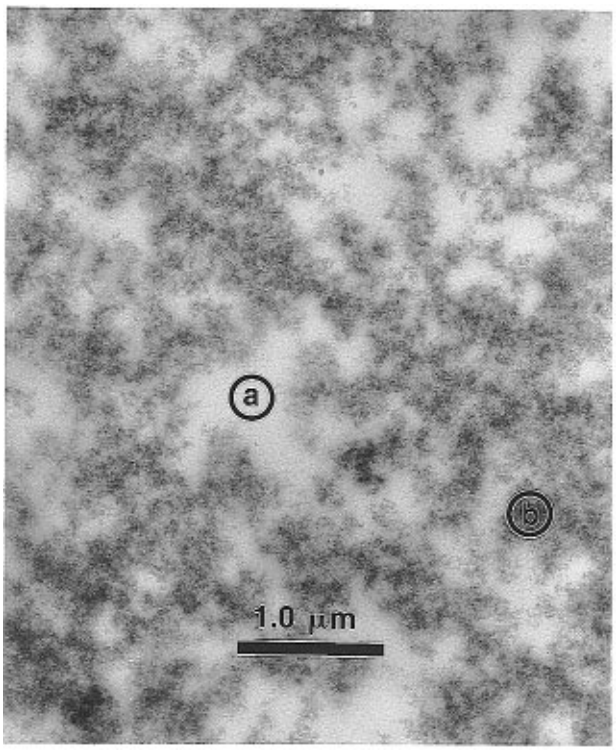

Figure 4. TEM micrograph of specimen HEA-2 (12 wt % SiO_2) with the regions labeled as described for Figure 3. This catalyst ratio produces a more uniform dispersion of the inorganic phase, with a dendritic or fractal-like morphology observed uniformly throughout the specimen.

3. Transmission Electron Microscopy. The study of organic/inorganic IPNs is greatly facilitated by TEM, for although these materials are optically transparent they have a microstructure in the submicron range. The contrast mechanism in the TEM of amorphous blends usually originates from differences in mass thickness (density times thickness). Since the thickness of the sample is approximately uniform for the microtomed specimens we have prepared, the contrast observed is attributed to density differences between the phases. In the IPN materials studied the organic polymer and SiO_2-rich phases are sufficiently different in density to produce good intrinsic contrast in the TEM.

The "ungrafted" HEA series show large differences in the morphology by TEM. In images of HEA-1 (Figure 3) and HEA-2 (Figure 4), the lighter regions labeled "a" are the organic-rich phases and the darker regions labeled "b" are the SiO_2-rich phases. In this series, the size of the SiO_2-rich domains is greater than or equal to the nominal sample thickness (600−900 Å), and the different regions are easily identified. As the SiO_2 phase becomes more finely dispersed in the organic matrix, as shown for HEA-4 (Figure 5), the domains become small relative to the sample thickness. The TEM image, which is a 2-dimensional projection, for very finely dispersed materials is therefore limited to stating an upper limit on the domain size and providing a rough measure of sample uniformity over a large area. It is difficult to discuss the interconnectivity of the material, since the image is the result of superposition of many layers of substructure. The morphology of each sample will now be described in more detail with regard to the above information.

For HEA-1, gross phase separation has occurred and the sample is very nonuniform, as shown in Figure 3.

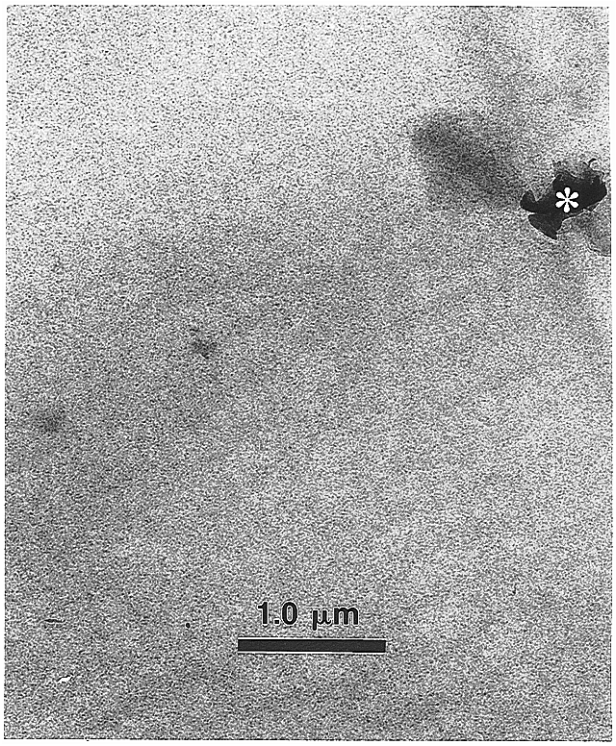

Figure 5. TEM micrograph of sample HEA-4. The SiO_2 content of this material, 16 wt %, was similar to that of HEA-2, but the morphology produced at this catalyst ratio is much finer. The same magnification is shown, compared to Figures 3 and 4, so that the uniformity of the specimen is adequately portrayed. The white star indicates a larger feature extraneous to the specimen used a focusing aid for this very low contrast image.

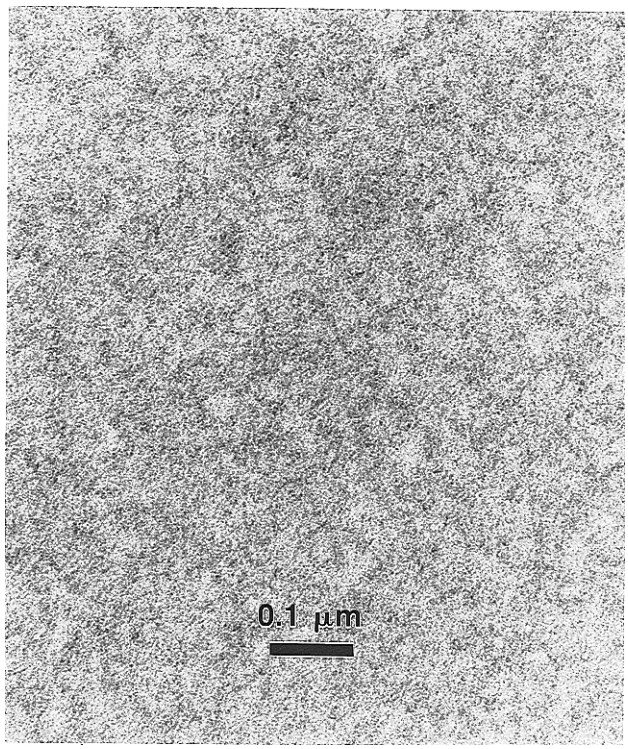

Figure 6. TEM micrograph of sample HEA-4 at a higher magnification, to better illustrate the finely dispersed morphology.

The region shown attempts to portray the wide range of morphology observed, from regions that are almost SiO_2 free (labeled "a") to regions that have low SiO_2 content and a fine fractal-like structure to regions which contain very large agglomerates (>1.0 μm) of inorganic material (labeled "b"). The TGA results on this material revealed SiO_2 contents from 0.10 to 0.23; this large degree of variation reflects the inhomogeneity of HEA-1 compared to the other samples in the series. For HEA-2, a fractal structure is seen with a size range of SiO_2-rich areas from 100 to 3000 Å, as shown in Figure 4. The SiO_2-rich domains are linked together in a dendritic morphology of larger scale. The specimen has good uniformity over large areas like that shown in Figure 4, although areas as large as 0.5 μm exist which contain little inorganic material. The morphology of HEA-3 was very similar to that shown in Figure 4 for HEA-2, although the domains of SiO_2 appeared to have more rounded edges. The similarity is not surprising since the HF/TEOS concentration for these two materials is very similar, as given in Table 1.

A much different morphology of very finely dispersed SiO_2 was observed for both HEA-4 and HEA-5. A TEM micrograph for a typical region of HEA-4 is shown in Figure 5, at the same magnification as shown in Figures 3 and 4 for HEA-1 and HEA-2, respectively, so that a direct comparison of the morphology size scale and uniformity can be made. Although the glass content of these materials is almost identical to that in HEA-2 and HEA-3 (12−16% SiO_2 as shown in Table 1), the morphology is entirely different. The white star in Figure 5 and subsequent figures is adjacent to a slightly larger feature that was used as a focusing aid for this type of specimen. We note that the regions shown in Figures 3−5 were typical of each specimen after multiple areas were carefully examined. Greater detail on this type of finely dispersed IPN was gained at higher magnification, shown for HEA-4 in Figure 6. Although the resolution is limited by the sample thickness, a grainy texture with fairly high contrast on a fine scale is observed for HEA-4, and the size scale is <100 Å. The texture seen in the IPN shown in Figure 6 is much coarser than that observed for either the carbon-coated grid or for a control of pure organic polymer[20] containing no SiO_2 and cannot be attributed to these factors.

The "grafted" B series was less distinctive in character by TEM as shown in the results in Figures 7 and 8 for B-2 and B-7, respectively, as compared to HEA-4 (Figure 6). Less contrast on a fine scale implies that the B series samples are more phase mixed and that the interfaces may be more diffuse than in the HEA series. This fine structure may be a result of the grafting between the organic and inorganic phases. The overall glass content is also lower, 5% for the B series compared to 12−16% for the HEA series, which makes imaging of the B series more difficult. B-2 has a mottled appearance of ~0.1 μm scale superimposed on a finer texture, as shown in Figure 7. The dark stripe through the center of the image is due to a thickness variation from microtoming. The texture of B-7 is finer and more uniform, as shown in Figure 8, where the size scale is smaller than 100 Å. Although the dispersion of the SiO_2 appears to be fairly uniform, there may be too little glass present to definitively image this type of specimen. The texture of B-7 is only slightly coarser than that observed for a pure organic polymer containing no SiO_2, as was previously published in our parallel study of organic/inorganic IPNs made from epoxy resin.[20] Regions shown in

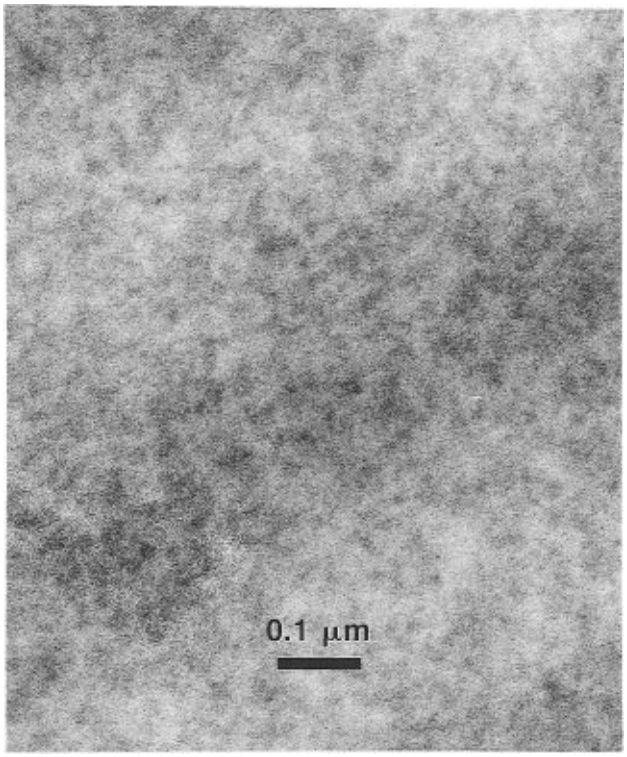

Figure 7. Typical morphology of the "grafted" specimen B-2, as seen by TEM, showing a mottled texture of ~0.1 μm size scale superimposed on a finer texture.

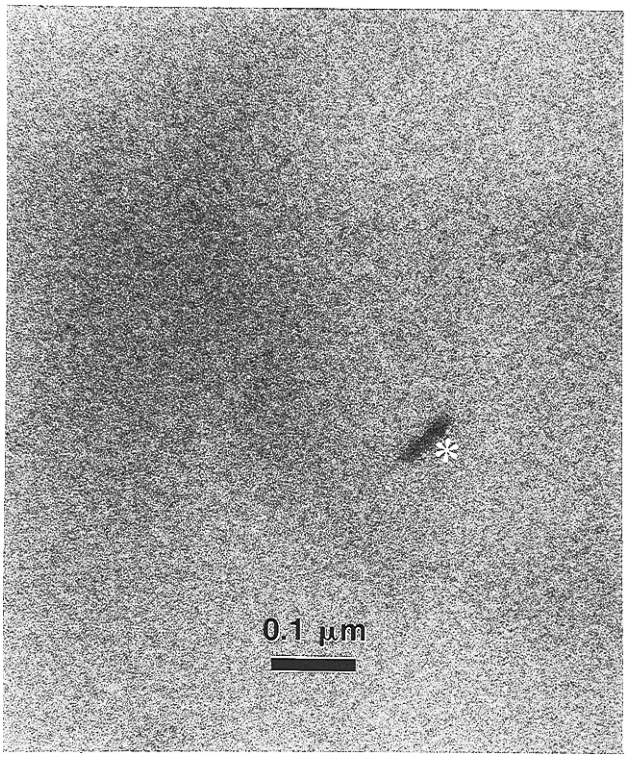

Figure 8. Typical morphology of the "grafted" specimen B-7, as seen by TEM, showing a very finely dispersed texture.

Figures 7 and 8 were typical of each specimen after multiple areas were carefully examined.

Conclusions

The influence of synthetic variables on the structure and morphology of organic/inorganic hybrid materials has been demonstrated for interpenetrating polymer networks of SiO_2 and acrylate polymers. The variables studied included the catalyst concentration for the sol−gel polymerization and the effect of grafting between the organic and inorganic phases. These variables were used to investigate the role of relative polymerization rate and degree of mixing between the two phases on the final morphology.

A combination of scattering and microscopy techniques was found to be very useful to characterize the IPN morphology. In the "ungrafted" IPNs (HEA-series), SANS and SAXS results for samples with the lowest level of sol−gel catalyst (HEA-1 and HEA-2) gave power law scattering over a wide angular range, which is consistent with a dendritic structure. In addition, analysis of the scattering in the Porod region suggested that relatively sharp boundaries exist between the organic and inorganic phases. For samples with a higher level of HF catalyst, and a "faster" sol−gel polymerization (HEA-4 and HEA-5), the scattering shows a much smaller size scale and suggests that more diffuse interfacial regions exist between the two phases. This is qualitatively in agreement with the TEM results, where an increase in the rate of sol−gel hydrolysis relative to the rate of conversion from vinyl monomer to polymer for "ungrafted" HEA-series produced a change from a dendritic structure, with diffuse edges of the SiO_2 phase and a broad size range of 300−3000 Å (HEA-2) to a finely divided morphology and a characteristic size scale of ~100 Å (HEA-4 and HEA-5).

The effect of grafting between the organic and inorganic phases was studied in the B series of samples, where covalent bonds exist between the sol−gel and vinyl components during the polymerization. The phase separation in these smaples is substantially weaker, with evidence of considerable mixing between the two phases from the scattering behavior in the power law region. The morphology from TEM is consistent with this finding, although the size scale is too small to resolve directly by the TEM method.

In summary, the different morphologies produced upon empirically changing the relative rates of polymerization are dramatic and one would predict that the mechanical, thermal, and electrical properties would be exceptionally different. We do not know at this time which morphology is preferable, and this may depend on the end use of the material. The presence of covalent bonds between the organic and inorganic phases as the polymerization proceeds, to produce a "grafted" IPN, may significantly influence the properties of these hybrid materials, as well, and merits more attention as these new materials are further developed.

CM950417H